FEBS Letters 555 (2003) 116–121 FEBS 27771

Minireview

Translocons, thermodynamics, and the folding of membrane proteins

Stephen H. White*

Department of Physiology and Biophysics and the Program in Macromolecular Structure, University of California at Irvine, Med. Sci. I-D346, Irvine, CA 92697-4560, USA

Received 25 August 2003; accepted 1 September 2003

First published online 16 October 2003

Edited by Gunnar von Heijne, Jan Rydström and Peter Brzezinski

Abstract Recent three-dimensional structures of helical membrane proteins present new challenges for the prediction of structure from amino acid sequence. Membrane proteins reside stably in a thermodynamic free energy minimum after release into the membrane's bilayer fabric from the translocon complex. This means that structure prediction is primarily a problem of physical chemistry. But the folding processes within the translocon must also be considered. A distilled overview of the physical principles of membrane protein stability is presented, and extended to encompass translocon-assisted folding.

Key words: Integral membrane protein; Protein folding; Structure prediction

1. Introduction

Bacteriorhodopsin [1], comprised of seven transmembrane (TM) helices packed neatly into a bundle (Fig. 1A), is generally taken as the archetypal membrane protein (MP). Its apparent simplicity has encouraged the belief that MP structure prediction should be relatively easy to accomplish by first identifying TM segments using hydropathy plots (reviewed in [2]) and then applying helix-packing constraints [3]. This optimistic assessment is gravely challenged by the 3D structure of the ClC chloride channel [4], shown in Fig. 1B. The jumble of helices buried within the membrane mocks bacteriorhodopsin's simplicity. Not only do the 17-odd helices vary greatly in length and tilt, some form TM structures using end-to-end arrangements in the manner of the aquaporin family of transporters (reviewed in [5]). Hydropathy plots utterly fail to identify the complex topology correctly. This failure is not limited to the ClC channel alone, as shown by the 3D structure of the KvAP voltage-gated potassium channel [6]. The S1–S4 voltage sensing region is not comprised of the simple TM helices surmised from hydropathy plot analyses. Rather, this region appears to be dominated by a helical hairpin arrangement that can move within the lipid bilayer in response to changes of membrane potential. These new structures force us to abandon the plot-and-pack structure prediction paradigm.

How can we develop a new paradigm for MP structure prediction? We can begin by addressing two fundamental issues of MPs: physical stability and biological assembly. Constitutive α-helical MPs are assembled in membranes by means of a translocation/insertion process that involves physical engagement of a ribosome with a translocon complex [7–11]. After release into the membrane's bilayer fabric and disassembly of the ribosome–translocon machine, a MP resides stably in a thermodynamic free energy minimum (evidence reviewed in [12,13]). This means that the prediction of MP structure from amino acid sequence is, in large measure, a problem of physical chemistry, albeit a complex one. Physical influences that shape MP structure include interactions of the polypeptide chains with water, each other, the bilayer hydrocarbon core, the bilayer interfaces, and cofactors (Fig. 1A). Several recent reviews [13–15] provide extensive discussions of the evolution, structure, and thermodynamic stability of MPs. My purpose here is to provide a distilled overview of the physical principles underlying MP stability and to extend the discussion to encompass the other fundamental issue, the biological assembly of MPs. I focus primarily on α-helical MPs, but the thermodynamic principles also apply to β-barrel MPs (reviewed in [16]).

2. Physical determinants of MP stability: the bilayer milieu

Two influences are paramount in shaping the MP structure. First, as implied in Fig. 1C, the membrane's bilayer fabric has two chemically distinct regions: hydrocarbon core (HC) and interfaces (IFs). Interfacial structure and chemistry must be important, because the specificity of protein signaling and targeting by membrane-binding domains could not otherwise exist [17]. Second, the high energetic cost of dehydrating the peptide bond, as when transferring it to a non-polar phase, causes it to dominate structure formation [18]. The only permissible TM structural motifs of MPs are α-helices and β-barrels, because internal H-bonding ameliorates this cost.

Because membranes must be in a fluid state for normal cell function, only the structure of fluid (L_α-phase) bilayers is relevant to understanding how membranes mold proteins. But atomic-resolution images of fluid membranes are precluded due to their high thermal disorder. Nevertheless, useful structural information can be obtained from multilamellar

*Fax: (1)-949-824 8540.
E-mail address: blanco@helium.biomol.uci.edu (S.H. White).

Abbreviations: MP, membrane protein; TM, transmembrane; HC, hydrocarbon core of a lipid bilayer; IF, interfacial region of a lipid bilayer; PC, phosphatidylcholine; POPC, palmitoyloleoylphosphatidylcholine; WW, Wimley–White

0014-5793/03/$22.00
doi:10.1016/S0014-5793(03)01153-0

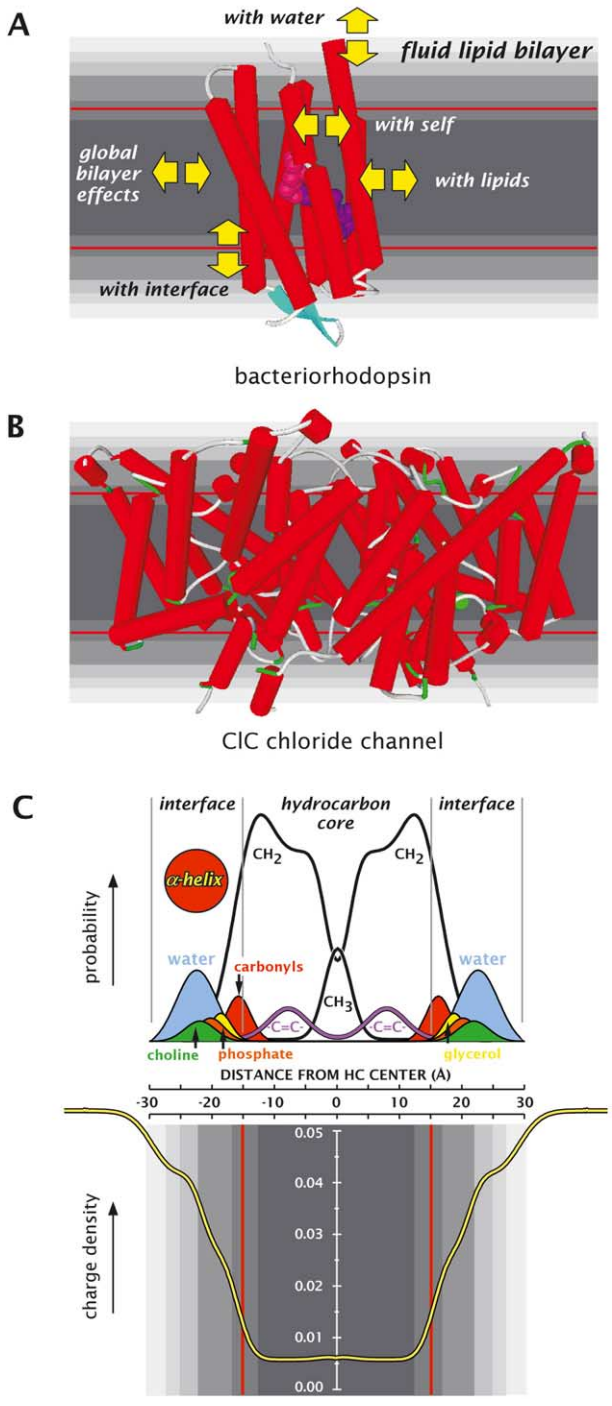

Fig. 1. The structures of two of strikingly different α-helical MPs and of a fluid lipid bilayer. A: Schematic structure of bacteriorhodopsin embedded in a lipid bilayer constructed using PDB coordinates 1C3W. The various interactions of the polypeptide that affect the 3D structure are shown. B: Schematic structure of the ClC chloride channel constructed using PDB coordinates 1OTS. C: Liquid-crystallographic structure of a fluid DOPC lipid bilayer [21] and its computed polarity profile [22]. The figure is adapted from reviews by White and Wimley [13,22,52].

bilayers (liquid crystals) dispersed in water or deposited on surfaces. Their 1D crystallinity perpendicular to the bilayer plane allows the distribution of matter along the bilayer normal to be determined by combined X-ray and neutron diffraction measurements (liquid crystallography; reviewed in [19,20]). The resulting 'structure' consists of a collection of time-averaged probability distribution curves of water and lipid component groups (carbonyls, phosphates, etc.), representing projections of 3D motions onto the bilayer normal. Fig. 1C shows the liquid-crystallographic structure of an L_α-phase dioleoylphosphatidylcholine (DOPC) bilayer [21].

Three features of this structure are important. First, the widths of the probability densities reveal the great thermal disorder of fluid membranes. Second, the combined thermal thicknesses of the interfaces (defined by the distribution of the waters of hydration) is about equal to the 30 Å thickness of the HC. The thermal thickness of a single IF (~15 Å) can easily accommodate an α-helix parallel to the membrane plane. The common cartoons of bilayers that assign a diminutive thickness to the bilayer IFs are thus misleading. Third, the thermally disordered IFs are highly heterogeneous chemically. A polypeptide chain in an IF must experience dramatic variations in environmental polarity over a short distance due to the steep changes in chemical composition, as illustrated by the yellow curve in the lower half of Fig. 1C [22]. As the regions of first contact, the IFs are especially important in the folding and insertion of non-constitutive MPs, such as diphtheria toxin, and to the activity of surface-binding enzymes, such as phospholipases. But, for reasons discussed below, they must also be important in translocon-assisted folding of MPs.

3. Physical determinants of MP stability: energetics of peptides in bilayers

Experimental exploration of the stability of intact MPs is problematic due to their general insolubility. One approach to stability is to 'divide and conquer' by studying the membrane interactions of fragments of MPs, i.e. peptides. Because MPs are equilibrium structures, folding and stability can be examined by constructing equilibrium thermodynamic pathways [13], described in detail elsewhere [13]. In brief, my laboratory employs a four-step model, which is a logical combination of the earlier three-step model of Jacobs and White [23] and the two-stage model of Popot and Engelman [24] in which TM helices are first 'established' across the membrane and then assembled into functional structures (helix association; reviewed in [25]). Although these pathways do not mirror the actual biological assembly process of MPs, they are nevertheless useful for guiding biological experiments, because they provide a thermodynamic context within which biological processes must proceed. Recent studies, discussed below, suggest that energetics derived from the four-step model are closely related to the process of translocon-assisted folding.

In the four-step model, the free energy reference state is taken as the unfolded protein in an IF. But this state cannot actually be achieved with MPs because of the solubility problems. Nor can it be achieved with small non-constitutive membrane-active peptides, such as melittin, because binding usually induces secondary structure (partitioning–folding coupling). It can be defined for phosphatidylcholine (PC) interfaces by means of an experiment-based interfacial free energy (hydrophobicity) scale [26] derived from partitioning into palmitoyloleoylphosphatidylcholine (POPC) bilayers of tri- and pentapeptides [23,26] that have no secondary structure in the aqueous or interfacial phases. This scale (Fig. 2A), which includes the peptide bonds as well as the sidechains,

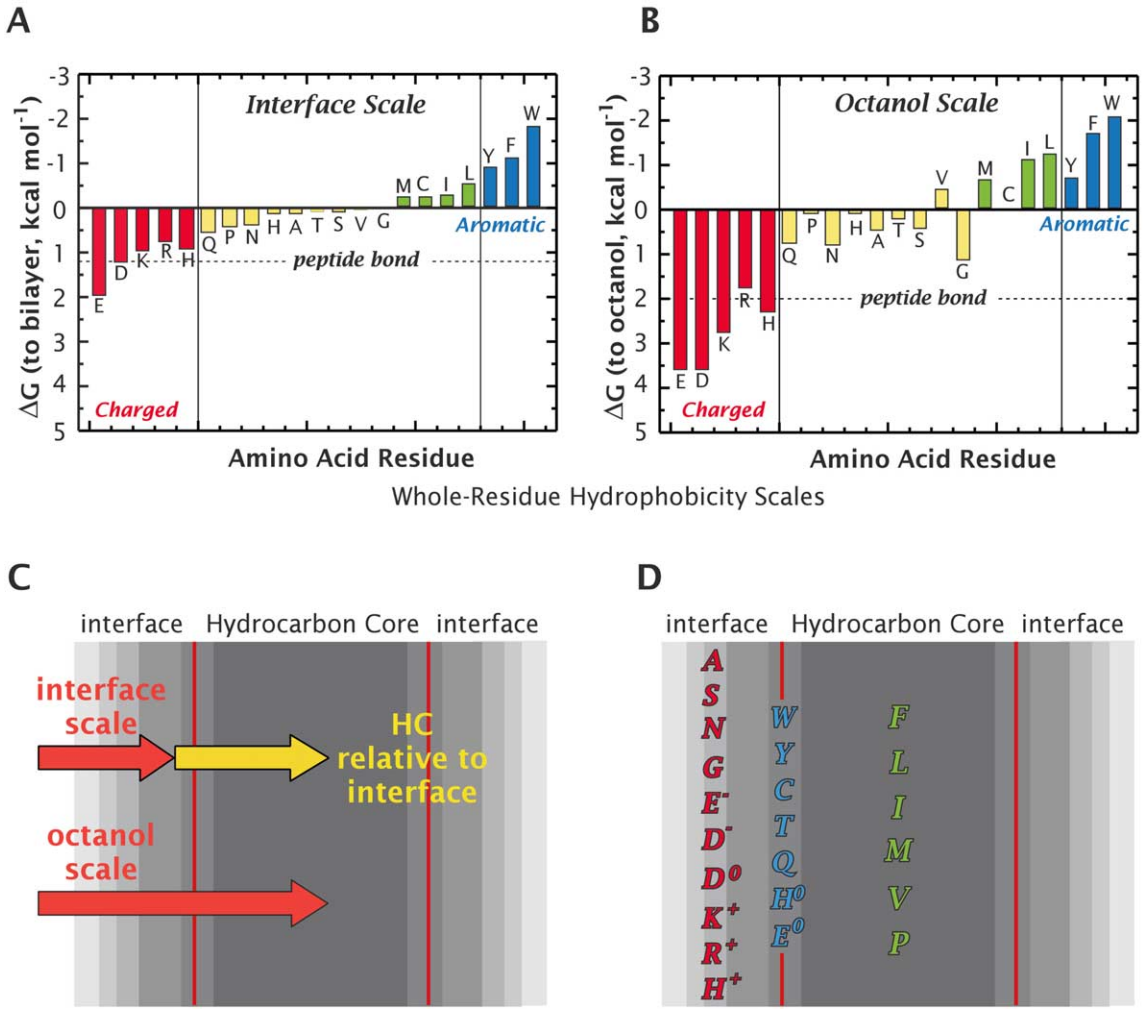

Fig. 2. Summary of experiment-based hydrophobicity scales that are useful for understanding MP stability and translocon-assisted folding. A: The WW interfacial hydrophobicity scale determined from measurements of the partitioning of short peptides into PC vesicles [26]. B: The WW octanol hydrophobicity scale determined from the partitioning of short peptides into *n*-octanol [38] that accurately predicts the stability of TM helices [36]. The free energy values along the abscissa are ordered in the same manner as in panel A. C: The basis for deriving the octanol-interface scale ($\Delta G_{oct-IF} = \Delta G_{oct} - \Delta G_{IF}$) from the scales shown in panels A and B. Numerical values for all of the scales can be obtained at http://blanco.biomol.uci.edu/hydrophobicity_scales.html. D: The octanol-interface scale divides the natural amino acid residues into three classes based upon their relative propensities for the hydrocarbon core and the membrane interface. These correlate well with the helical hairpin turn propensity [42], Fig. 3B.

allows calculation of the virtual free energy of transfer of an unfolded chain into an IF. For peptides that cannot form regular secondary structure, such as the antimicrobial peptide indolicidin, the scale predicts observed free energies of transfer with remarkable accuracy [27]. This validates it for computing virtual partitioning free energies of proteins into PC IFs. Similar scales are needed for other lipids and lipid mixtures.

The high cost of interfacial partitioning of the peptide bond [26], 1.2 kcal mol^{-1}, explains the origin of partitioning–folding coupling and also why the interface is a potent catalysis of secondary structure formation. Wimley et al. [28] showed for interfacial β-sheet formation that H-bond formation reduces the cost of peptide partitioning by about 0.5 kcal mol^{-1} per peptide bond. The folding of melittin into an amphipathic α-helix on POPC membranes involves a per-residue reduction of about 0.4 kcal mol^{-1} [29]. The folding of other peptides seems to involve smaller per-residue values [30,31]. The cumulative effect of these relatively small per-residue free energy reductions can be very large when tens or hundreds of residues are involved.

The energetics of TM helix stability also depend critically on the partitioning cost of peptide bonds. Determination of the energetics of TM α-helix insertion, which is necessary for predicting structure, is difficult because non-polar helices tend to aggregate in both aqueous and interfacial phases [32]. The broad energetic issues are clear [33], however. Computational studies [34,35] suggest that the transfer free energy ΔG_{CONH} of a non-H-bonded peptide bond from water to alkane is +6.4 kcal mol^{-1}, compared to only +2.1 kcal mol^{-1} for the transfer free energy ΔG_{Hbond} of an H-bonded peptide bond. The per-residue free energy cost of disrupting H-bonds in a membrane is therefore about 4 kcal mol^{-1}. A 20 AA TM helix would thus cost 80 kcal mol^{-1} to unfold within a membrane, which explains why unfolded polypeptide chains cannot exist in a TM configuration.

As discussed in detail elsewhere [15,36], ΔG_{Hbond} sets the threshold for TM stability as well as the so-called decision

level in hydropathy plots [2]. The free energy of transfer of non-polar sidechains dramatically favors helix insertion, while the transfer cost of the helical backbone dramatically disfavors insertion. For example [15], the favorable (hydrophobic effect) free energy for the insertion of the single membrane-spanning helix of glycophorin A [37] is estimated to be −36 kcal mol^{-1}, whereas the cost ΔG_{bb} of dehydrating the helix backbone is +26 kcal mol^{-1}. The net free energy ΔG_{TM} favoring insertion is thus −10 kcal mol^{-1}. Uncertainties in the per-residue cost of backbone insertion will have a major effect on estimates of TM helix stability, the interpretation of hydropathy plots, and the establishment of the minimum value of sidechain hydrophobicity required for stability. An uncertainty of 0.5 kcal mol^{-1}, for example, would cause an uncertainty of about 10 kcal mol^{-1} in ΔG_{TM}!

What is the most likely estimate of ΔG_{Hbond}? The practical number is the cost $\Delta G^{helix}_{glycyl}$ of transferring a single glycyl unit of a polyglycine α-helix into the bilayer HC. Electrostatic calculations [35] and the octanol partitioning study of Wimley et al. [38] suggested that $\Delta G^{helix}_{glycyl} = +1.25$ kcal mol^{-1}, which is the basis for the calculation of ΔG_{bb}. The cost of transferring a random-coil glycyl unit into *n*-octanol [38] is +1.15 kcal mol^{-1}, which suggested that the *n*-octanol whole-residue hydrophobicity scale [13] (Fig. 2B) derived from the partitioning data of Wimley et al. [38] might be a good measure of $\Delta G^{helix}_{glycyl}$. This hypothesis was borne out by a study [36] of known TM helices cataloged in the MPtopo database of MPs of known topology [39], accessible via the World Wide Web at http://blanco.biomol.uci.edu/mptopo. This study showed that +1.15 kcal mol^{-1} is indeed the best estimate of $\Delta G^{helix}_{glycyl}$. Using this value, TM helices for MPs of known 3D structure could be identified with better than 99% accuracy in the 2001 edition of MPtopo. The whole-residue octanol scale can thus be taken as an accurate hydrophobicity scale for amino acid residues in α-helices. This scale also includes free energy values for protonated and deprotonated forms of Asp, Glu, and His. In addition, Wimley et al. [40] determined the free energies of partitioning salt bridges into octanol, which are believed to be good estimates for partitioning into membranes [36]. This has led to the augmented Wimley–White (aWW) hydrophobicity scale [36] that forms the basis for a useful hydropathy-based tool, MPEx, for analyzing MP protein stability. MPEx is available as an on-line java applet at http://blanco.biomol.uci.edu/mpex.

The WW experiment-based whole-residue hydrophobicity scales [26,36,38], Fig. 2A (ΔG_{IF}) and Fig. 2B (ΔG_{oct}), provide a solid starting point for understanding MP stability. When the two scales are used together (Fig. 2C), one can estimate the preference of a polypeptide segment for HC as an α-helix relative to the membrane interface as an unfolded chain. The 'octanol-interface' scale, $\Delta G_{oct-IF} = \Delta G_{oct} - \Delta G_{IF}$, divides the amino acid residues into three groups (Fig. 2D): strongly IF-preferring, strongly HC-preferring, and those that are borderline ($|\Delta G_{oct-IF}| \leq 0.25$ kcal mol^{-1}). The octanol-interface scale provides insights into translocon-assisted folding [41–43].

4. Connecting translocon-assisted folding to the WW hydrophobicity scales

The vast literature on translocon-assisted MP folding has been reviewed extensively in the past several years [7–11]. Here it is sufficient to note that the signal recognition particle targets nascent ribosome-bound membrane and secreted proteins to the translocon (Sec61p) complex, whereupon membrane integration and folding occurs, provided that the nascent protein has at least one run of amino acids with sufficient hydrophobicity to form a TM helix/stop-transfer sequence. Otherwise, the protein is secreted across the membrane. The ribosome–translocon complex is shown schematically in the upper half of Fig. 3A, based upon an image reconstruction at 17 Å resolution [44]. Two points of view regarding translocon-assisted membrane integration, discussed extensively by Johnson [8], are shown schematically in the lower half of the figure.

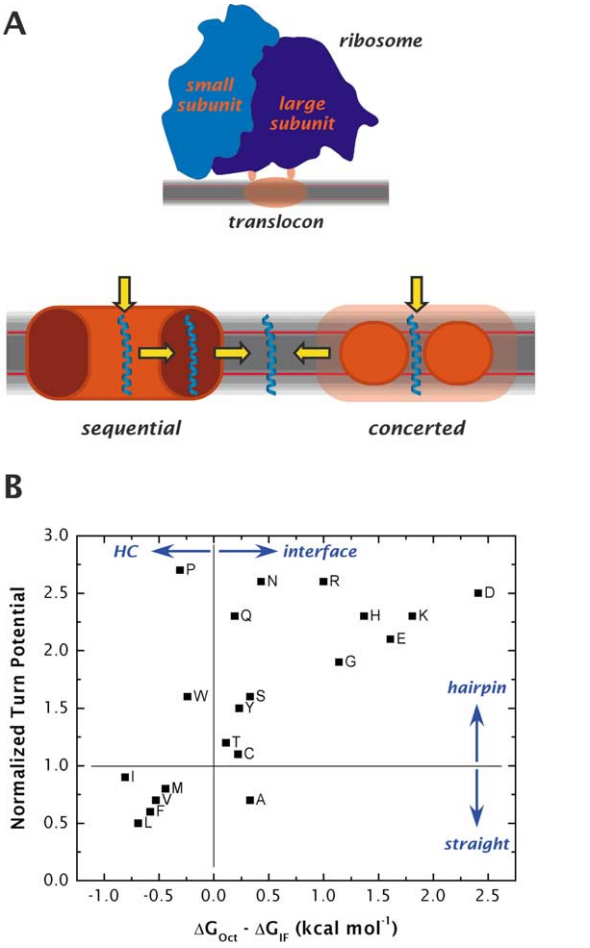

Fig. 3. Schematic of translocon-assisted folding and its relationship to the octanol-interface hydrophobicity scale. A: A sketch of the translocon–ribosome complex assembled in a lipid bilayer (upper image) and two schemes for TM helix incorporation into lipid bilayers by the translocon (lower images). The upper sketch is derived from a cryo-EM image reconstruction at 17 Å resolution [44]. The sequential scheme envisions that MP folding takes place largely within a large ribosome tunnel prior to integration into the bilayer. The concerted scheme, which is strongly supported by experimental evidence, envisions simultaneous interactions of the growing peptide chain with the lipid bilayer and the translocon complex. See text for discussion. B: A plot of the normalized turn propensity for helical hairpin formation [42] versus the octanol-interface hydrophobicity scale (Fig. 2). There is a clear correlation between the turn propensity and octanol-interface hydrophobicity. Those residues that favor the conversion of a long (∼40 AA), single-spanning polyleucine TM helix into a helical hairpin (two TM helices separated by a tight turn) are generally the same ones that favor the membrane interface. See text for discussion.

The 'sequential' point of view visualizes the translocon as having a large tunnel of about 50 Å diameter into which the nascent protein chain is secreted during folding, preparatory to insertion into the lipid bilayer via a passageway through the wall of the translocon. A crucial feature of this scheme is that the ribosome must make a tight seal with the translocon in order to prevent ion leakage. However, there is a growing body of evidence that the alternate 'concerted' scheme, in which the translocon complex and the lipid work together, is more likely. The present vagueness of the scheme is indicated schematically in Fig. 3A (lower right) by means of a transparent translocon overlay on the lipid bilayer. Two low-resolution (~15 Å) images of ribosome–translocon assemblies indicate significant gaps between the ribosome and translocon [44,45], which eliminates the possibility of a tight seal. It appears that sealing is provided in some way by the nascent peptide within the translocon itself. Site-specific photo-cross-linking studies [46] show that the nascent chain can cross-link with lipids well before the termination of translation, implying that the growing chain interacts with both the translocon and neighboring lipids during folding. Heinrich et al. [47] concluded that the integration of TM domains occurs through a lipid-partitioning process as a result of the TM segment being in contact with the lipid as soon as it arrives in the translocon channel. But integration into the membrane can occur only if a polypeptide segment is sufficiently hydrophobic.

What is the minimum hydrophobicity required for a 20-amino acid segment to be integrated into the lipid bilayer? Chen and Kendall [48] answered this question for *Escherichia coli* by attaching artificial stop-transfer sequences to alkaline phosphatase, which is a water-soluble protein that is normally secreted across the membrane. Potential stop-transfer sequences (21 AA) composed of Leu and Ala in various ratios were introduced into an internal position of the enzyme by cassette mutagenesis. The threshold value of hydrophobicity for integration was found to be 16 Ala and five Leu. This is exactly the threshold predicted by the WW octanol-based hydrophobicity scale, as shown by Jayasinghe et al. [36]. This establishes a tight relationship between the WW octanol scale and translocon-assisted folding.

There is also evidence for a relationship between the WW interfacial scale and translocon-mediated folding. Nilsson and von Heijne [49] made the interesting observation that a $Leu_{39}Val$ hydrophobic sequence introduced into leader peptidase was incorporated into the membranes of dog pancreas microsomes as a single TM helix. The fact that this helix is twice the length of the typical TM helix strongly supports the idea of early contact of the growing chain with membrane lipids. The more striking observation, however, was that the introduction of a single proline into the center of the $Leu_{39}Val$ segment caused it to be inserted as a helical hairpin. That is, the proline induced the formation of two TM segments separated by a tight turn. Expanding on this observation, Monné et al. [41,42] established a turn propensity scale by introducing one or two of each of the natural amino acids into the center of a 40-residue polyleucine sequence. The residues with a favorable turn potential were found to be, in decreasing order, Pro, Asn, Arg, Asp, His, Gln, Lys, Glu, and Gly. Except for Pro, which commonly occurs within TM helices of ordinary length [50], these are the residues in the WW octanol-interface scale (Fig. 2D) that have a strong interface preference. Another misfit is Ala, which has a low turn potential but a significant interfacial preference. The relationship between turn potential and the octanol-interface scale is shown in Fig. 3B. The correlation coefficient between the scales is 0.67, meaning that there is not a strict linear relationship. This is not surprising because turn potential is affected by the length of the long polyleucine segment and the number of residues of a given type introduced into the segment's center [42]. For example, a single proline placed in the center of a $Leu_{29}Val$ sequence does not induce hairpin formation.

A closer connection between turn potential and the WW octanol-interface scale was disclosed by studies of turn-induction by runs of Ala residues placed in the center of polyleucine segments [43]. A run of about four alanines was found to induce helical hairpins efficiently in hydrophobic segments as short as 34 residues. Furthermore, glycosylation mapping revealed a slight preference of alanine for the membrane interface, consistent with the WW octanol-interface scale.

These various studies support strongly the idea that the translocon and lipid bilayer work in concert to integrate hydrophobic segments into membranes, which strengthens the lipid-partitioning model of Rapoport and colleagues [47]. In addition, the studies establish a direct link between the WW hydrophobicity scales and translocon-assisted folding. An early study [51] of the relationship between hydrophobicity and translocon-mediated integration found that popular hydrophobicity scales of the time could not predict accurately the hydrophobic threshold for stop-transfer activity. The reason is now understood [36]. Prior to the WW experiment-based scales, no hydrophobicity scale took into account the cost of dehydrating the helix backbone. As result, sidechain-only scales dramatically overpredictrd TM helices in MPs of known structure. If one thinks of the threshold for insertion as the mid-point of a Boltzmann probability curve, sidechain-only scales will cause the apparent threshold to have a positive ΔG, rather than the expected value of zero. Indeed, Sääf et al. [51] found the mean per-residue hydrophobicity threshold to be approximately +1.5 kcal mol^{-1}, which is about the cost of dehydrating the peptide bond. Had the partitioning cost of the peptide bond been appreciated and taken into account, the threshold then would have been very close to $\Delta G = 0$. Now that accurate experiment-based scales are available that account for both interfacial and hydrocarbon core partitioning, it will be possible to design more finely tuned TM helices for probing translocon-assisted folding.

Acknowledgements: The research from my laboratory described in this review was carried out over a period of years by a number of talented postdoctoral students, including Drs. Michael Wiener, William Wimley, Alex Ladokhin, Kalina Hristova, and Sajith Jayasinghe. I thank Mr. Michael Myers for his excellent editorial assistance and for the management of my laboratory. Discussions of translocon-assisted folding with Dr. Gunnar von Heijne and his laboratory have been invaluable. This work was supported in part by grants from the National Institutes of Health, GM46823 and GM68002.

References

[1] Lanyi, J.K. and Schobert, B. (2003) J. Mol. Biol. 328, 439–450.
[2] White, S.H. (1994) in: Membrane Protein Structure: Experimental Approaches (White, S.H., Ed.), pp. 97–124, Oxford University Press, New York.
[3] Bowie, J.U. (1999) Protein Sci. 8, 2711–2719.

[4] Dutzler, R., Campbell, E.B., Cadene, M., Chait, B.T. and MacKinnon, R. (2002) Nature 415, 287–294.
[5] Stroud, R.M., Miercke, L.J.W., O'Connell, J., Khademi, S., Lee, J.K., Remis, J., Harries, W., Robles, Y. and Akhavan, D. (2003) Curr. Opin. Struct. Biol. 13, 424–431.
[6] Jiang, Y.X., Lee, A., Chen, J.Y., Ruta, V., Cadene, M., Chait, B.T. and MacKinnon, R. (2003) Nature 423, 33–41.
[7] Bibi, E. (1998) Trends Biochem. Sci. 23, 51–55.
[8] Johnson, A.E. and van Waes, M.A. (1999) Annu. Rev. Cell Dev. Biol. 15, 799–842.
[9] Driessen, A.J.M., Manting, E.H. and van der Does, C. (2001) Nat. Struct. Biol. 8, 492–498.
[10] Dalbey, R.E. and von Heijne, G. (2002) Protein Targeting Transport and Translocation, Academic Press, New York.
[11] Pfeffer, S. (2003) Cell 112, 507–517.
[12] Lemmon, M.A. and Engelman, D.M. (1994) Q. Rev. Biophys. 27, 157–218.
[13] White, S.H. and Wimley, W.C. (1999) Annu. Rev. Biophys. Biomol. Struct. 28, 319–365.
[14] Popot, J.-L. and Engelman, D.M. (2000) Annu. Rev. Biochem. 69, 881–922.
[15] White, S.H., Ladokhin, A.S., Jayasinghe, S. and Hristova, K. (2001) J. Biol. Chem. 276, 32395–32398.
[16] Wimley, W.C. (2003) Curr. Opin. Struct. Biol. 13, 404–411.
[17] Hurley, J.H. and Misra, S. (2000) Annu. Rev. Biophys. Biomol. Struct. 29, 49–79.
[18] Liu, Y. and Bolen, D.W. (1995) Biochemistry 34, 12884–12891.
[19] White, S.H. and Wiener, M.C. (1995) in: Permeability and Stability of Lipid Bilayers (Disalvo, E.A. and Simon, S.A., Eds.), pp. 1–19, CRC Press, Boca Raton, FL.
[20] White, S.H. and Wiener, M.C. (1996) in: Membrane Structure and Dynamics (Merz, K.M. and Roux, B., Eds.), pp. 127–144, Birkhäuser, Boston, MA.
[21] Wiener, M.C. and White, S.H. (1992) Biophys. J. 61, 434–447.
[22] White, S.H. and Wimley, W.C. (1998) Biochim. Biophys. Acta 1376, 339–352.
[23] Jacobs, R.E. and White, S.H. (1989) Biochemistry 28, 3421–3437.
[24] Popot, J.-L. and Engelman, D.M. (1990) Biochemistry 29, 4031–4037.
[25] Curran, A.R. and Engelman, D.M. (2003) Curr. Opin. Struct. Biol. 13, 412–417.
[26] Wimley, W.C. and White, S.H. (1996) Nat. Struct. Biol. 3, 842–848.
[27] Ladokhin, A.S. and White, S.H. (2001) J. Mol. Biol. 309, 543–552.
[28] Wimley, W.C., Hristova, K., Ladokhin, A.S., Silvestro, L., Axelsen, P.H. and White, S.H. (1998) J. Mol. Biol. 277, 1091–1110.
[29] Ladokhin, A.S. and White, S.H. (1999) J. Mol. Biol. 285, 1363–1369.
[30] Wieprecht, T., Beyermann, M. and Seelig, J. (1999) Biochemistry 38, 10377–10387.
[31] Li, Y., Han, X. and Tamm, L.K. (2003) Biochemistry 42, 7245–7251.
[32] Wimley, W.C. and White, S.H. (2000) Biochemistry 39, 4432–4442.
[33] Roseman, M.A. (1988) J. Mol. Biol. 201, 621–625.
[34] Ben-Tal, N., Sitkoff, D., Topol, I.A., Yang, A.-S., Burt, S.K. and Honig, B. (1997) J. Phys. Chem. B 101, 450–457.
[35] Ben-Tal, N., Ben-Shaul, A., Nicholls, A. and Honig, B. (1996) Biophys. J. 70, 1803–1812.
[36] Jayasinghe, S., Hristova, K. and White, S.H. (2001) J. Mol. Biol. 312, 927–934.
[37] Segrest, J.P., Jackson, R.L., Marchesi, V.T., Guyer, R.B. and Terry, W. (1972) Biochem. Biophys. Res. Commun. 49, 964–969.
[38] Wimley, W.C., Creamer, T.P. and White, S.H. (1996) Biochemistry 35, 5109–5124.
[39] Jayasinghe, S., Hristova, K. and White, S.H. (2001) Protein Sci. 10, 455–458.
[40] Wimley, W.C., Gawrisch, K., Creamer, T.P. and White, S.H. (1996) Proc. Natl. Acad. Sci. USA 93, 2985–2990.
[41] Monné, M., Hermansson, M. and von Heijne, G. (1999) J. Mol. Biol. 288, 141–145.
[42] Monné, M., Nilsson, I.M., Elofsson, A. and von Heijne, G. (1999) J. Mol. Biol. 293, 807–814.
[43] Nilsson, I.M., Johnson, A.E. and von Heijne, G. (2003) J. Biol. Chem. 278, 29389–29393.
[44] Morgan, D.G., Ménétret, J.-F., Neuhof, A., Rapoport, T.A. and Akey, C.W. (2002) J. Mol. Biol. 324, 871–886.
[45] Beckmann, R., Spahn, C.M.T., Eswar, N., Helmers, J., Penczek, P.A., Sali, A., Frank, J. and Blobel, G. (2001) Cell 107, 361–372.
[46] Mothes, W., Heinrich, S.U., Graf, R., Nilsson, I.M., von Heijne, G., Brunner, J. and Rapoport, T.A. (1997) Cell 89, 523–533.
[47] Heinrich, S.U., Mothes, W., Brunner, J. and Rapoport, T.A. (2000) Cell 102, 233–244.
[48] Chen, H. and Kendall, D.A. (1995) J. Biol. Chem. 270, 14115–14122.
[49] Nilsson, I.M. and von Heijne, G. (1998) J. Mol. Biol. 284, 1185–1189.
[50] Williams, K.A. and Deber, C.M. (1991) Biochemistry 30, 8919–8923.
[51] Sääf, A., Wallin, E. and von Heijne, G. (1998) Eur. J. Biochem. 251, 821–829.
[52] White, S.H. and Wimley, W.C. (1994) Curr. Opin. Struct. Biol. 4, 79–86.